

Finite-time Lyapunov exponents in time-delayed nonlinear dynamical systems

Kazutaka Kanno* and Atsushi Uchida†

Department of Information and Computer Sciences, Saitama University, 255 Shimo-okubo, Sakura-ku, Saitama City, Saitama, 338-8570, Japan

(Received 3 August 2013; revised manuscript received 19 January 2014; published 25 March 2014)

We introduce a method for the calculation of finite-time Lyapunov exponents in time-delayed nonlinear dynamical systems. We apply the method to the Mackey-Glass model with time-delayed feedback. We investigate the standard deviation of the probability distribution of the finite-time Lyapunov exponents when the finite time or the delay time is changed. It is found that the standard deviation decreases in a power-law scaling with the exponent ~ 0.5 as the finite time or the delay time is increased. Similar results are obtained for the finite-time Lyapunov spectrum.

DOI: [10.1103/PhysRevE.89.032918](https://doi.org/10.1103/PhysRevE.89.032918)

PACS number(s): 05.45.Pq, 05.45.Jn, 05.45.Gg, 42.65.Sf

I. INTRODUCTION

Nonlinear dynamical systems with time-delayed feedback show very rich complex behaviors because the systems are considered as infinite-dimensional systems [1,2]. Neuronal networks, electronic circuits, and laser systems are typical examples of time-delayed dynamical systems [3–6]. Recently, the use of time-delayed dynamical systems has been reported for applications of fast physical random number generators [7], reservoir computing [8], and optical secure communications [9,10]. The estimation of the dimensionality and the entropy of the dynamical system is important for these applications.

The dimensionality and the entropy of dynamical systems can be quantified with Lyapunov exponents [1,2,11–13]. Lyapunov exponents characterize average growth rates of small perturbations to an orbit of an attractor in the phase space and a positive value of the maximum Lyapunov exponent indicates deterministic chaos. Many methods for the calculation of the Lyapunov exponents have been well established for both discrete and continuous dynamical systems [14–21]. One of the most trusted methods for the estimation of the Lyapunov exponent in continuous dynamical systems is the use of linearized model equations that govern the evolution of small perturbations to an orbit in the phase space [14–16].

The Lyapunov exponents are asymptotic in time and averaged over an attractor. On the contrary, finite-time Lyapunov exponents have been proposed to investigate finite-time behaviors on a chaotic attractor [22,23]. The finite-time Lyapunov exponents are exponential growth rates of small perturbations on the attractor for finite-time intervals. They have been also known as local Lyapunov exponents [24,25] and finite-size Lyapunov exponents [26], where the growth rates are measured in a finite size in the phase space, instead of a finite time. The analysis of the finite-time behaviors is quite important for the classification of chaotic dynamics [27,28], controlling local chaotic dynamics [29], unpredictability of physical random number generators [30], and information capacity of reservoir computing [8]. The finite-time Lyapunov exponents may significantly differ from the average Lyapunov exponents, depending on phase-space locations. The standard deviation

of the probability distribution of the finite-time Lyapunov exponents is one of the useful quantities to identify statistical property of the finite-time Lyapunov exponents [22]. However, the finite-time Lyapunov exponents in time-delayed dynamical systems have not been reported yet, because the construction of the phase space for the calculation of the finite-time Lyapunov exponents has not been clearly understood.

In this study, we introduce a method for the calculation of the finite-time Lyapunov exponents in time-delayed nonlinear dynamical systems. We treat a time-delayed system as a finite-dimensional system by discretizing time-delayed components with a short time step and derive a calculation method of the finite-time Lyapunov exponents by linearizing the system. We apply the method to the Mackey-Glass model with time-delayed feedback and investigate the dependence of the standard deviation of the probability distribution of the finite-time Lyapunov exponents on the finite time and the delay time. We also investigate the characteristics of the finite-time Lyapunov spectrum.

II. CALCULATION METHOD FOR FINITE-TIME LYAPUNOV EXPONENTS IN TIME-DELAYED DYNAMICAL SYSTEMS

We derive a calculation method for the finite-time Lyapunov exponents for any time intervals in time-delayed dynamical systems. A time-delayed dynamical system with N -state variables $\mathbf{x}^T(t) = [x_1(t), x_2(t), \dots, x_N(t)]$, where T represents transpose, is described as follows:

$$\frac{dx_j(t)}{dt} = f_j[\mathbf{x}(t), \mathbf{x}(t - \tau)], \quad (1)$$

where $j = 1, 2, \dots, N$, $\mathbf{x}(t - \tau)$ is the time-delayed component and τ is the delay time. The dynamical system with time-delayed feedback is considered as an infinite-dimensional system since the state of Eq. (1) is determined by the variable \mathbf{x} on the continuous-time interval $[t, t - \tau]$. The state can be approximated by a new variable $\mathbf{y}(t)$ that consists of $M + 1$ samples of the variable $\mathbf{x}(t)$ taken at a small interval $h = \tau/M$ [1,2], i.e., $\mathbf{y}^T(t) = [\mathbf{x}^T(t), \mathbf{x}^T(t - h), \mathbf{x}^T(t - 2h), \dots, \mathbf{x}^T(t - Mh)]$. This approximation indicates that an N -dimensional system with time-delayed feedback is considered as an $N(M + 1)$ -dimensional ordinary dynamical system. The dynamical evolution of Eq. (1) is transformed into the following map by

*s11dm001@mail.saitama-u.ac.jp

†auchida@mail.saitama-u.ac.jp

discretization with a small time step h :

$$\mathbf{y}(t+h) = \mathbf{F}[\mathbf{y}(t)]. \quad (2)$$

The time evolution from $\mathbf{y}(t)$ to $\mathbf{y}(t+h)$ is considered for the calculation of finite-time Lyapunov exponents. The variable $\mathbf{y}(t)$ is constructed for every τ step [i.e., $\mathbf{y}(t)$, $\mathbf{y}(t+\tau)$, $\mathbf{y}(t+2\tau)$, ...] to represent spatiotemporal behaviors [31–33] and to calculate the maximum Lyapunov exponent [1,2]. However, the introduction of Eq. (2) enables us to investigate the calculation of finite-time Lyapunov exponents for the short time step h .

To calculate the Lyapunov exponents, we consider a small (linear) perturbation $\delta\mathbf{x}(t) = \mathbf{x}(t) - \bar{\mathbf{x}}(t)$, where $\delta\mathbf{x}^T(t) = [\delta x_1(t), \delta x_2(t), \dots, \delta x_N(t)]$, from an original trajectory $\bar{\mathbf{x}}(t)$. The evolution of the perturbation for Eq. (1) is governed by the following linearized equation [1,6,12,13]:

$$\frac{d\delta\mathbf{x}(t)}{dt} = \mathbf{J}_t\delta\mathbf{x}(t) + \mathbf{J}_{t-\tau}\delta\mathbf{x}(t-\tau). \quad (3)$$

The matrices \mathbf{J}_t and $\mathbf{J}_{t-\tau}$ are $N \times N$ matrixes whose i - j elements are $\partial f_i/\partial x_j(t)$ and $\partial f_i/\partial x_j(t-\tau)$, respectively. It is worth noting that the variables $x_j(t)$ and time-delayed variables $x_j(t-\tau)$ are treated as independent variables to derive Eq. (3) [1]. We consider a new variable for perturbation $\delta\mathbf{y}(t)$ in an $N(M+1)$ -dimensional phase space, i.e., $\delta\mathbf{y}^T(t) = [\delta\mathbf{x}^T(t), \delta\mathbf{x}^T(t-h), \delta\mathbf{x}^T(t-2h), \dots, \delta\mathbf{x}^T(t-Mh)]$. The evolution of $\delta\mathbf{y}(t)$ is described by the following equation by linearizing Eq. (2):

$$\delta\mathbf{y}(t+h) = \mathbf{F}_D[\mathbf{y}(t)]\delta\mathbf{y}(t), \quad (4)$$

where \mathbf{F}_D is the $N(M+1) \times N(M+1)$ Jacobian matrix of \mathbf{F} . The formula of \mathbf{F}_D is shown in Appendix A. In continuous dynamical systems, the integration of Eqs. (1) and (3) is required to obtain the tangent map $\mathbf{Y}(t)$, which takes the initial variables $\delta\mathbf{y}(0)$ into the time-evolved variables $\delta\mathbf{y}(t)$, i.e., $\delta\mathbf{y}(t) = \mathbf{Y}(t)\delta\mathbf{y}(0)$, where $\mathbf{Y}(t) = \mathbf{F}_D[\mathbf{y}(t-h)]\mathbf{F}_D[\mathbf{y}(t-2h)] \cdots \mathbf{F}_D[\mathbf{y}(0)]$. The average Lyapunov exponents can be obtained as the logarithm of the eigenvalues of $\lim_{t \rightarrow \infty} [\mathbf{Y}^T(t)\mathbf{Y}(t)]^{1/2t}$ [14–16,18]. The finite-time Lyapunov exponents for any finite times L can also be obtained as the logarithm of the eigenvalues of $[\mathbf{Y}^T(L)\mathbf{Y}(L)]^{1/2L}$. Reorthogonalization and normalization is required by using QR decomposition [14–16].

The norm of $\delta\mathbf{y}(t)$ has been often used for the calculation of Lyapunov exponents in continuous-time dynamical systems, instead of $\mathbf{Y}(t)$ [1,6,12,13]. By integrating Eqs. (1) and (3) simultaneously, we can obtain the evolution of $\delta\mathbf{y}(t)$ and $\delta\mathbf{x}(t)$ in $[t, t+\tau]$. The norm $d(t)$ of $\delta\mathbf{y}(t)$ is defined as follows:

$$d(t) = \|\delta\mathbf{y}(t)\| = \sqrt{\sum_{j=1}^N \sum_{i=0}^M |\delta x_j(t-ih)|^2}. \quad (5)$$

The finite-time Lyapunov exponents for any time intervals $L = kh$ (k is an integer and h is the integration time step) can be defined as follows:

$$\lambda_f(L) = \frac{1}{L} \ln \frac{d(t+L)}{d(t)} = \frac{1}{kh} \sum_{j=1}^k \ln \frac{d(t+jh)}{d[t+(j-1)h]}. \quad (6)$$

Note that $\delta\mathbf{x}(t)$ needs to be normalized by the norm $d(t)$ for each integration time step h to maintain a small amount of $\delta\mathbf{x}(t)$.

We use Eqs. (5) and (6) for the calculation of the finite-time Lyapunov exponents in the following sections. The calculation method of the finite-time Lyapunov exponents from the eigenvalues of the Jacobian matrix \mathbf{F}_D will be described in Appendix A.

III. NUMERICAL RESULTS OF FINITE-TIME LYAPUNOV EXPONENTS IN THE MACKEY-GLASS MODEL

First we consider the finite-time property of the maximum Lyapunov exponent in this section. The finite-time property of the second (and more) Lyapunov exponents can be calculated by using other sets of Eq. (4) and orthogonalization of $\delta\mathbf{y}(t)$ [22], which will be described in Sec. IV.

We used the Mackey-Glass model [34] to show the validity of our method:

$$\frac{dx(t)}{dt} = \frac{ax(t-\tau)}{1+x^b(t-\tau)} - cx(t), \quad (7)$$

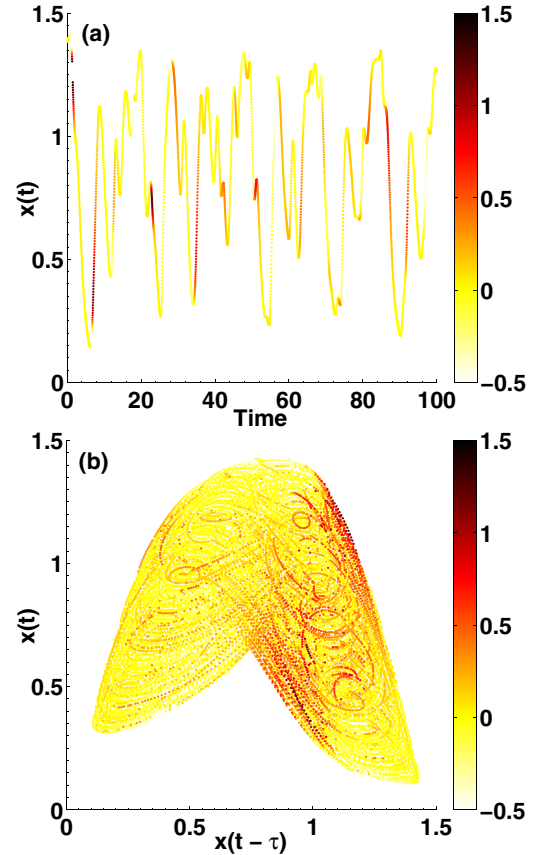


FIG. 1. (Color online) Finite-time Lyapunov exponents plotted on (a) the temporal waveform and (b) the two-dimensional projection of the chaotic attractor in the Mackey-Glass model. Red points indicate large positive values of the finite-time Lyapunov exponents. The integration time step is set to $h = 0.02$. The delay time $\tau = 5$ and the finite time for the calculation $L = 0.02 (= h)$ are used for the numerical simulations.

where $x(t - \tau)$ represents the time-delayed variable, τ is the delay time, and a , b , and c are the fixed parameters. From Eq. (3), the Mackey-Glass model of Eq. (7) is linearized with a new variable for perturbation $\delta x(t) = x(t) - \bar{x}(t)$ from an original trajectory $\bar{x}(t)$ as follows:

$$\frac{d\delta x(t)}{dt} = -c\delta x(t) + \frac{a + a(1-b)x^b(t-\tau)}{[1 + x^b(t-\tau)]^2} \delta x(t-\tau). \quad (8)$$

A time series of the perturbation δx is obtained from numerical integration of both Eqs. (7) and (8). The finite-time Lyapunov exponents of Eq. (6) can be calculated from the time evolution of the norm of Eq. (5).

We set the parameter values to $a = 2$, $b = 10$, and $c = 1$, respectively. The integration time step h is set to 0.02 in our numerical simulations for the Mackey-Glass model. The delay time is set to $\tau = 5$. For these parameter values, the Mackey-Glass system is approximated by a 251-dimensional ordinary dynamical system (i.e., $N = 1$, $M = \tau/h = 250$).

Figure 1 shows the temporal waveform and the finite-time Lyapunov exponents projected on the two-dimensional chaotic attractor of the Mackey-Glass model. The finite time L is

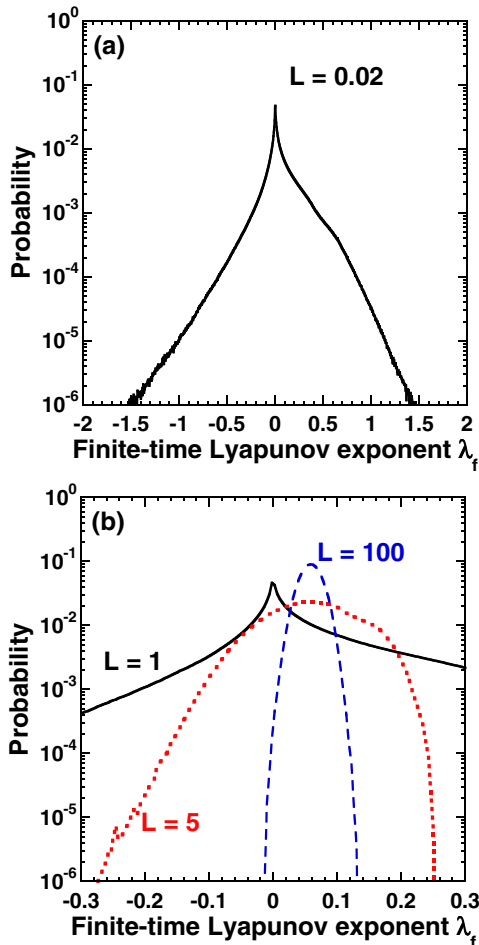


FIG. 2. (Color online) Probability distributions of the finite-time Lyapunov exponents for the delay time $\tau = 5$. The finite times are set to (a) $L = 0.02$ and (b) $L = 1, 5$, and 100 , respectively. The maximum Lyapunov exponent is $\lambda_{\max} = 0.058$. Note that the horizontal axis of (b) is expanded from that of (a).

set to be 0.02 ($=h$). Red points represent large values of the finite-time Lyapunov exponents. The finite-time Lyapunov exponents on the temporal waveform $x(t)$ are changed in time as shown in Fig. 1(a). We found that the finite-time Lyapunov exponents depend on the locations of the chaotic attractor in the phase space in Fig. 1(b).

Figure 2(a) shows the probability distribution of the finite-time Lyapunov exponents over the chaotic attractor for $L = 0.02$ ($=h$), as used in Fig. 1. The finite-time Lyapunov exponents show the distribution ranging from -1.5 to 1.5 . The maximum Lyapunov exponent λ_{\max} , which is the mean value of the finite-time Lyapunov exponents, is 0.058 . Compared with λ_{\max} , the finite-time Lyapunov exponent has larger absolute values. When the finite time L is increased, different probability distributions are obtained, as shown in Fig. 2(b). The delay time $\tau = 5$ is used and three examples are shown in Fig. 2(b) ($L < \tau$, $L = \tau$, and $L > \tau$). We found that the distributions become narrower as the finite time L is increased in Fig. 2(b). We also found that the peak value of the probability distributions for $L = 5$ and 100 matches λ_{\max} . The peak value is shifted from 0 to λ_{\max} at $L \approx \tau$ when L is increased. The shape of the distribution is drastically changed from the skewed distribution [the case for $L = 1$ in Fig. 2(b)] to the Gaussian distribution (the case for $L = 100$). The change in the probability distributions is observed for other values of τ .

We calculated the standard deviation of the probability distribution of finite-time Lyapunov exponents to quantitatively evaluate the dependence of the distribution on the finite time L . Figure 3 shows the standard deviation as a function of L for the delay times $\tau = 5, 10$, and 20 . We found that the standard deviation decreases for all the cases and the decay of the standard deviation obeys a power law in terms of the finite time L , denoted by L^{-p} . The curve for $\tau = 20$ has a little distortion at $L \approx \tau$, which results from the transition

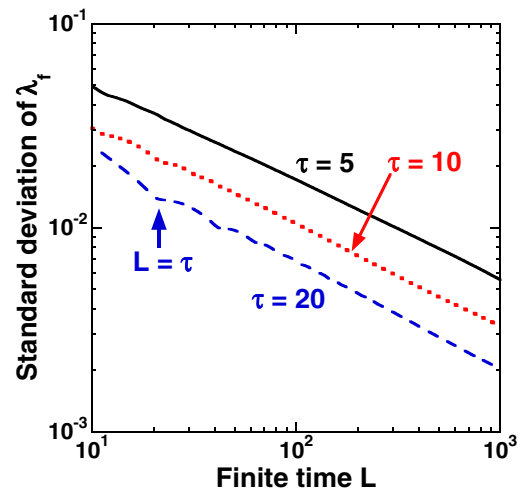


FIG. 3. (Color online) Standard deviation of the probability distribution of the finite-time Lyapunov exponents as a function of the finite time L on the double-logarithmic plot. The delay times $\tau = 5, 10$, and 20 are used. The power-law scaling is found for all the cases, denoted by L^{-p} . The scaling exponents of $p = 0.48, 0.50$, and 0.51 are obtained for the delay times $\tau = 5, 10$, and 20 , respectively, in the range $20 \leq L \leq 1000$.

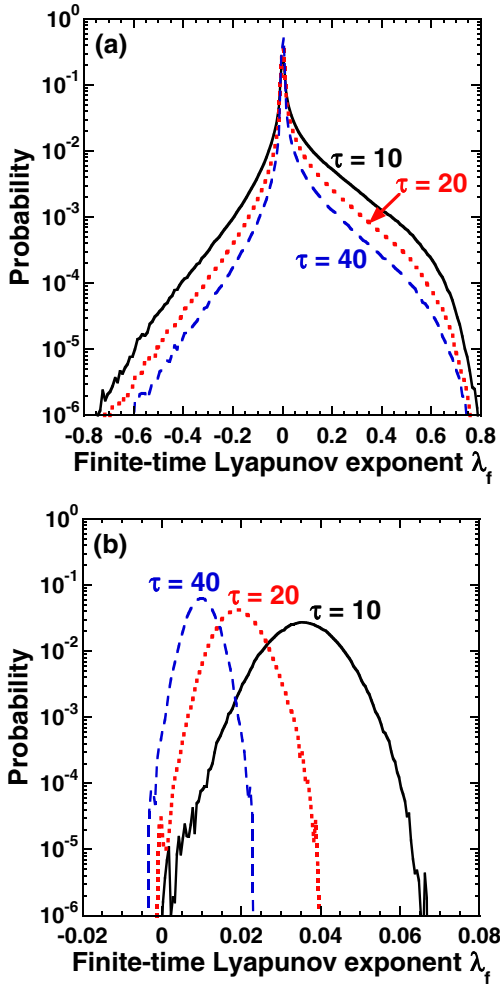


FIG. 4. (Color online) Probability distributions of the finite-time Lyapunov exponents for the finite times (a) $L = 1$ ($L < \tau$) and (b) $L = 200$ ($L > \tau$). The delay times $\tau = 10, 20,$ and 40 are used. The maximum Lyapunov exponents λ_{\max} are $0.036, 0.019,$ and 0.010 for $\tau = 10, 20,$ and 40 , respectively. The peak values of the distributions are located at λ_{\max} in (b) for $L > \tau$.

from the skewed distribution to the Gaussian distribution, as shown in Fig. 2(b). In the range of $L \approx \tau$, the peak value of the distribution shifts from 0 to λ_{\max} , which causes the distortion of the curve in Fig. 3. The scaling exponents $p = 0.48, 0.50,$ and 0.51 are obtained for $\tau = 5, 10,$ and 20 , respectively, by applying the least-squares method to the curves in Fig. 3. It has been reported in the literature that p ranges from 0.5 to 1.0 in ordinary dynamical systems without time-delayed feedback [22]. Our results show that a similar scaling exponent p can be obtained in the Mackey-Glass model with time-delayed feedback.

Next we investigate the dependence of the probability distribution of the finite-time Lyapunov exponent on the delay time τ . Figure 4 shows the probability distribution of the finite-time Lyapunov exponent for the delay times $\tau = 10, 20,$ and 40 . We set the finite times $L = 1$ and 200 for Figs. 4(a) and 4(b), respectively. The widths of the distributions become narrower with the increase of τ for both Figs. 4(a) and 4(b). The peak value remains the same at $\lambda_{\text{peak}} = 0$ in Fig. 4(a). On

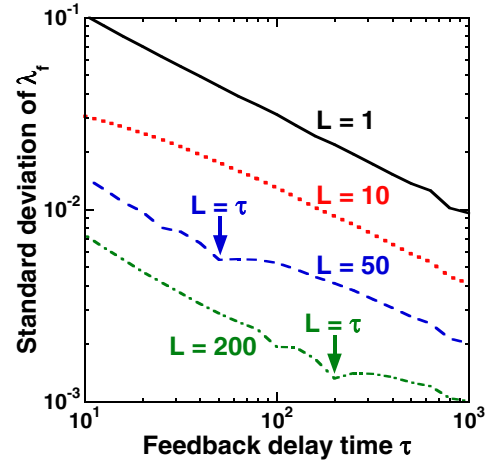


FIG. 5. (Color online) Standard deviation of the probability distribution of the finite-time Lyapunov exponent as a function of the delay time τ in the Mackey-Glass model on the double-logarithmic plot. The finite times $L = 1, 10, 50,$ and 200 are used. The power-law scaling is found for all the cases, denoted by τ^{-q} . The exponent of $q = 0.51$ is obtained for $L = 1$ in $10 \leq \tau \leq 1000$, $q = 0.50$ is obtained for $L = 10$ in $100 \leq \tau \leq 1000$, $q = 0.59$ and 0.46 are obtained for $L = 50$ in $10 \leq \tau \leq 50$ and $200 \leq \tau \leq 1000$, respectively, and $q = 0.54$ is obtained for $L = 200$ in $10 \leq \tau \leq 200$.

the contrary, the peak value corresponding to λ_{\max} is decreased when τ is increased in Fig. 4(b).

Figure 5 shows the standard deviation of the finite-time Lyapunov exponents as a function of the delay time τ . Both the horizontal and vertical axes are logarithmic scales, as in Fig. 3. The standard deviation decreases in a power-law scaling in terms of τ , denoted by τ^{-q} . For the cases of $L = 50$ and 200 , a power-law scaling is found in the range $\tau < L$. The scaling exponents are $q = 0.59$ and 0.54 for $L = 50$ and 200 , respectively. When τ exceeds L , the distribution changes from the Gaussian distribution to the skewed distribution. The power-law scaling cannot be observed in the transition between the two types of distributions. However, the power-law scaling is obtained again for larger τ . For example, the exponents of $q = 0.51$ and 0.50 are obtained for $L = 1$ and 10 for $\tau > L$, respectively. From these results, it is found that the standard deviation of the probability distribution of the finite-time Lyapunov exponents can be fitted with a power law in terms of the delay time τ except for the range of $L \approx \tau$. The scaling exponents are $q \approx 0.5$, as in the case of the scaling for the finite time L . Similar results are observed for another example of a time-delayed dynamical system, i.e., an optoelectronic time-delayed feedback system, as shown in the Appendix B.

IV. FINITE-TIME LYAPUNOV SPECTRUM

In the previous section, we considered the finite-time property of the maximum Lyapunov exponent. A set of n Lyapunov exponents can be obtained in an n -dimensional dynamical system, which is known as the Lyapunov spectrum. In this section, we consider the finite-time property of the second-largest and more Lyapunov exponents (i.e., Lyapunov spectrum) in the Mackey-Glass model. We investigate the

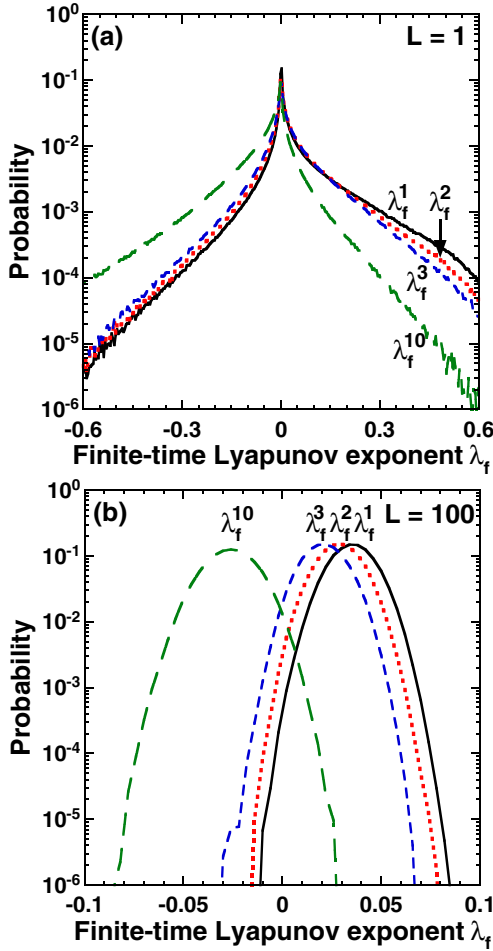


FIG. 6. (Color online) Probability distributions of the i th largest finite-time Lyapunov exponents λ_f^i , where $i = 1, 2, 3$, and 10 . The finite times $L = 1$ and 100 are used for (a) and (b), respectively. The black solid curve represents the maximum finite-time Lyapunov exponents λ_f^1 . The red dotted, blue dashed, and green long-dashed curves represent λ_f^2 , λ_f^3 , and λ_f^{10} , respectively. The delay time $\tau = 10$ is used.

standard deviation of the probability distribution of several finite-time Lyapunov exponents.

Figure 6 shows the probability distributions of four finite-time Lyapunov exponents λ_f^1 , λ_f^2 , λ_f^3 , and λ_f^{10} , where λ_f^i represents the i th largest finite-time Lyapunov exponents. The delay time of the Mackey-Glass model is set to $\tau = 10$, where five positive average Lyapunov exponents are obtained. The finite times $L = 1$ and 100 are used in Figs. 6(a) and 6(b), respectively. For $L < \tau$ in Fig. 6(a), the peaks of the four probability distributions are located at $\lambda_f^i \approx 0$. However, positive components of the probability distributions of the finite-time Lyapunov exponents are decreased and negative components are increased, as the index i is increased. On the contrary, for $L > \tau$ in Fig. 6(b), the peaks of the probability distributions are shifted to the negative direction as the index i is increased, even though the shapes of the distributions are almost the same (i.e., similar to the Gaussian distributions). In fact, the peaks are located at the average Lyapunov exponents for the i th largest Lyapunov exponents. We found

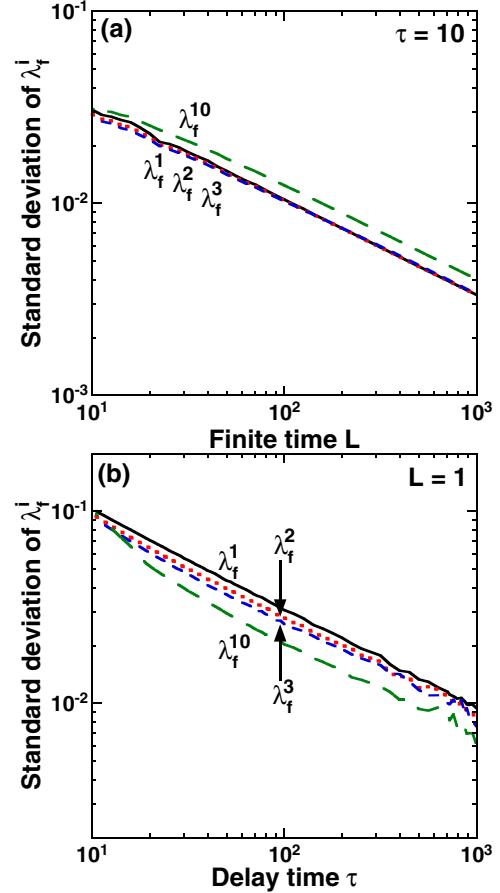


FIG. 7. (Color online) Standard deviation of the probability distribution of the i th largest finite-time Lyapunov exponents λ_f^i as functions of (a) the finite time L and (b) the delay time τ on the double-logarithmic plot. The black solid, red dotted, blue dashed, and green long-dashed curves represent λ_f^1 , λ_f^2 , λ_f^3 , and λ_f^{10} , respectively. (a) The scaling exponents $p = 0.49, 0.48, 0.47$, and 0.48 are obtained for λ_f^1 , λ_f^2 , λ_f^3 , and λ_f^{10} , respectively, by fitting the standard deviation to the power law L^{-p} in $20 \leq L \leq 1000$. The delay time $\tau = 10$ is fixed. (b) The scaling exponents $q = 0.51, 0.51, 0.51$, and 0.54 are obtained for λ_f^1 , λ_f^2 , λ_f^3 , and λ_f^{10} , respectively, by fitting to the power law τ^{-q} . The finite time $L = 1$ is fixed.

that the finite-time Lyapunov spectrum has similar probability distributions.

We also investigate the standard deviations of the probability distributions of the i th largest finite-time Lyapunov exponents λ_f^i as the finite time L or the delay time τ is changed. Figure 7(a) shows the standard deviations of the probability distributions of the finite-time Lyapunov exponents λ_f^1 , λ_f^2 , λ_f^3 , and λ_f^{10} when the finite time L is changed. The vertical and horizontal axes are logarithmic. The standard deviations for all the finite-time Lyapunov exponents obey the power-law scaling L^{-p} , as shown in Fig. 7(a). We can obtain the scaling exponents $p = 0.49, 0.48, 0.47$, and 0.48 for λ_f^1 , λ_f^2 , λ_f^3 , and λ_f^{10} , respectively, by fitting the standard deviations to the power law L^{-p} . Figure 7(b) shows the standard deviations of the probability distributions of λ_f^1 , λ_f^2 , λ_f^3 , and λ_f^{10} when the delay time τ is changed. Similarly, the standard deviations for all the finite-time Lyapunov exponents obey the power law τ^{-q} . The scaling

exponents are $q = 0.51, 0.51, 0.51$, and 0.54 for $\lambda_f^1, \lambda_f^2, \lambda_f^3$, and λ_f^{10} , respectively. Therefore, the power-law scaling with the exponent ~ 0.5 is found for the standard deviations of the probability distributions of the finite-time Lyapunov spectrum.

V. DEPENDENCE OF STANDARD DEVIATION ON DELAY-TIME DISCRETIZATION

The state variables $\mathbf{x}(t)$ within the delay time $[t - \tau, t]$ are discretized by the integration time step h to convert from an infinite-dimensional system to a finite-dimensional system, where the dimensionality is $N(M + 1)$ (N is the number of the variables for the original model and $M = \tau/h$). In this section, we investigate how many points of delay-time discretization are required for reliable estimation of the finite-time Lyapunov exponents in the Mackey-Glass model. We introduce a sampling time T_s for this calculation and the integration time step h is fixed to avoid the change in the original trajectory $\mathbf{x}(t)$, where $T_s \geq h$. The number of delay-time discretization is defined as $M' = \tau/T_s$ and the norm of the linearized equations are calculated by using M' instead of M (where $M' \leq M$). In this case, we consider the $N(M' + 1)$ -dimensional state variable $\delta \mathbf{y}^T(t) = [\delta \mathbf{x}^T(t), \delta \mathbf{x}^T(t - T_s), \delta \mathbf{x}^T(t - 2T_s), \dots, \delta \mathbf{x}^T(t - M'T_s)]$ by discretizing the original state variable $\mathbf{x}(t)$ in $[t - \tau, t]$ with the sampling time T_s . We change M' (or T_s) and investigate the characteristics of the probability distributions of the maximum finite-time Lyapunov exponent for different M' (or T_s). It is expected that larger M' (smaller T_s) results in more reliable estimation of the finite-time Lyapunov exponents.

Figure 8(a) shows the standard deviations of the probability distributions of the maximum finite-time Lyapunov exponents when M' is changed for $\tau = 6$ and 60 . The integration time step $h = 0.01$ is fixed. For $\tau = 6$, the standard deviation converges into a constant value (0.039) in the range of $M' \geq 8$. On the contrary, for $\tau = 60$, the standard deviation converges into a constant value (0.015) in the range of $M' \geq 80$. Therefore, it is required to increase the number of the points of the delay-time discretization as the delay time is increased to obtain correct estimation of the finite-time Lyapunov exponents.

Figure 8(b) shows the standard deviations of the probability distributions of the maximum finite-time Lyapunov exponents when T_s is changed. In this case, the standard deviations have constant values in the range of $T_s \leq 0.75$ for both delay times $\tau = 6$ and 60 . Therefore, the sampling time T_s needs to be less than a constant value (i.e., 0.75 in this example), regardless of the delay time, to obtain reliable estimation of the finite-time Lyapunov exponents.

VI. CONCLUSION

We introduced a method to calculate the finite-time Lyapunov exponents in time-delayed nonlinear dynamical systems. We calculated the probability distribution of the finite-time maximum Lyapunov exponents for the Mackey-Glass model and found that the shape of the distribution changes from skewed to Gaussian distributions as the finite time is increased. The transition of the two distributions occurs when the finite time is close to the delay time. The power-law scaling is observed for the standard deviation of the probability distribution of the finite-time Lyapunov exponents for both the finite time L and the delay time τ , except for the transition of the two distributions. Both of the scaling exponents p and q (L^{-p} and τ^{-q}) are close to 0.5. Similar characteristics of the probability distributions and the scaling exponents of the standard deviations are obtained for the finite-time Lyapunov spectrum.

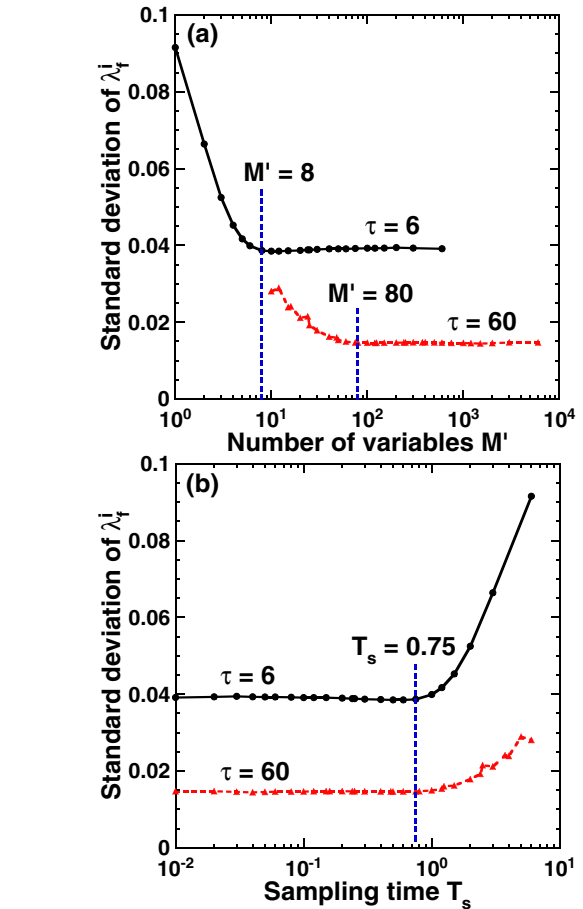


FIG. 8. (Color online) Standard deviation of the probability distribution of the finite-time Lyapunov exponents as functions of (a) the number of the discretized state variables M' ($M' = \tau/T_s$) and (b) the sampling time T_s for the discretization. The black solid and red dotted curves represent the delay times $\tau = 6$ and 60 , respectively. The integration time step $h = 0.01$ is fixed.

The finite-time Lyapunov exponents are good quantitative measures for the evaluation of unpredictability for random number generators with chaotic dynamics and for the evaluation of complexity in reservoir computing systems. Our method could be useful for these applications.

ACKNOWLEDGMENTS

We would like to thank Tohru Ikeguchi, Rajarshi Roy, Takaomi Shigehara, Angelo Vulpiani, and Kazuyuki Yoshimura for their fruitful comments. We acknowledge support from a Grant-in-Aid for Young Scientists and Management Expenses Grants from the Ministry of Education, Culture, Sports, Science and Technology in Japan. This work was supported in part by the Japan Society for the Promotion of Science research fellowship (Grant No. 25-8278).

APPENDIX A: DERIVATION OF THE JACOBIAN MATRIX USING THE EULER METHOD IN A CONTINUOUS-TIME DYNAMICAL SYSTEM

The Jacobian matrix F_D in Eq. (4) can be derived by discretizing a continuous-time dynamical system. The following discretized map can be obtained from Eq. (3) by using the Euler method:

$$\delta x(t+h) = (I + hJ_t)\delta x(t) + hJ_{t-\tau}\delta x(t-\tau), \quad (A1)$$

where h is the discretized time step and I is the $N \times N$ identity matrix. The variable of linear perturbation $\delta y(t+h)$ at time $t+h$ can be obtained from the mapping of F_D with the variable $\delta y(t)$ at time t as shown in Eq. (4). The Jacobian

matrix F_D can be described from Eq. (A1) as follows:

$$F_D[y(t)] = \begin{pmatrix} I + hJ_t & \mathbf{0} & \cdots & \mathbf{0} & hJ_{t-\tau} \\ I & \mathbf{0} & \cdots & \mathbf{0} & \mathbf{0} \\ & & \ddots & \ddots & \vdots \\ & & & & \mathbf{0} \\ \mathbf{0} & & & & I \end{pmatrix}, \quad (A2)$$

where F_D is the $N(M+1) \times N(M+1)$ matrix and $\mathbf{0}$ is the $N \times N$ zero matrix. The first column of F_D corresponds to Eq. (A1) and the other columns indicate shift operation of the components $\delta x(t-h), \delta x(t-2h), \dots$, and $\delta x[t-(M-1)h]$.

An example of F_D for the Mackey-Glass model is derived as follows. The Mackey-Glass model of Eq. (7) is linearized with a new variable for perturbation $\delta x(t) = x(t) - \bar{x}(t)$ from an original trajectory $\bar{x}(t)$ [Eq. (8) is rewritten]:

$$\frac{d\delta x(t)}{dt} = -c\delta x(t) + \frac{a + a(1-b)x^b(t-\tau)}{[1 + x^b(t-\tau)]^2} \delta x(t-\tau). \quad (A3)$$

After the discretization of Eq. (A3) by using the Euler method, the Jacobian matrix F_D for the Mackey-Glass model is described as follows:

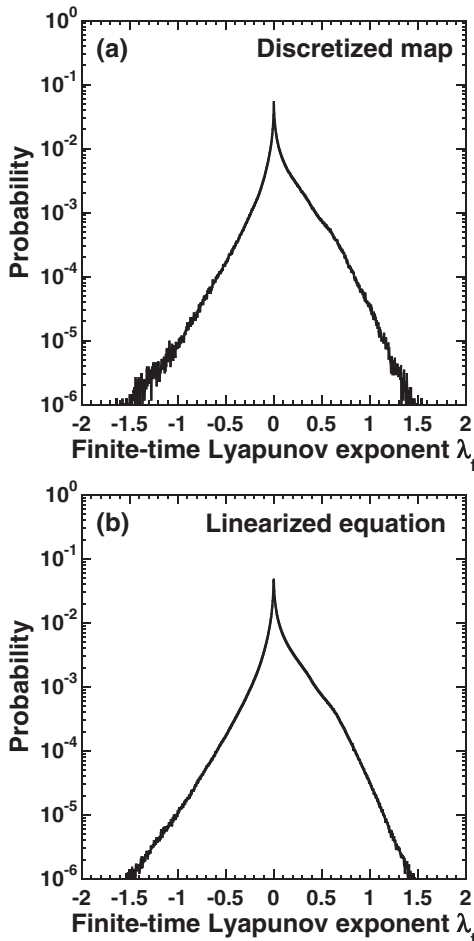


FIG. 9. Probability distribution of finite-time Lyapunov exponents obtained from (a) the discretized map F_D and (b) the norm of Eq. (5) by using the linearized equation [same as Fig. 2(a)]. The time step is set to $h = 0.02$.

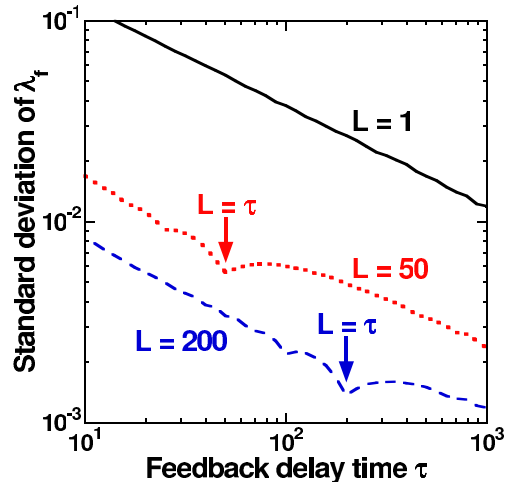


FIG. 10. (Color online) Standard deviation of the probability distribution of the finite-time Lyapunov exponents as a function of the delay time τ in the optoelectronic time-delayed feedback system [4,11]. The power-law scaling exponent q is obtained from fitting to τ^{-q} . The exponent $q = 0.50$ is obtained for $L = 1$ in $10 \leq \tau \leq 1000$. The exponents $q = 0.62$ and 0.45 are obtained for $L = 50$ in $10 \leq \tau \leq 50$ and $200 \leq \tau \leq 1000$, respectively. The exponent $q = 0.55$ is obtained for $L = 200$ in $10 \leq \tau \leq 200$.

$$\mathbf{F}_D[\mathbf{y}(t)] = \begin{pmatrix} 1 + hJ_t & 0 & \cdots & 0 & hJ_{t-\tau} \\ 1 & 0 & \cdots & 0 & 0 \\ & \ddots & \ddots & \vdots & \vdots \\ & & & 0 & 0 \\ 0 & & & 1 & 0 \end{pmatrix}, \quad (\text{A4})$$

$$J_t = -c, \quad (\text{A5})$$

$$J_{t-\tau} = \frac{a + a(1-b)x^b(t-\tau)}{[1 + x^b(t-\tau)]^2}, \quad (\text{A6})$$

where \mathbf{F}_D is the $(M+1) \times (M+1)$ matrix.

The finite-time Lyapunov exponents for any finite times L can be obtained as the logarithm of the eigenvalues of $[\mathbf{Y}^T(L)\mathbf{Y}(L)]^{1/2L}$, where $\mathbf{Y}(t)$ is the tangent map, i.e., $\mathbf{Y}(t) = \mathbf{F}_D[\mathbf{y}(t-h)]\mathbf{F}_D[\mathbf{y}(t-2h)] \cdots \mathbf{F}_D[\mathbf{y}(0)]$. The numerical results of the finite-time Lyapunov exponents calculated from $\mathbf{Y}(t)$ are shown in Fig. 9(a). The probability distribution of the finite-time Lyapunov exponents agrees well with that obtained from Eq. (6) with the norm $d(t)$ of $\delta \mathbf{y}(t)$ by using the linearized equation, as shown in Fig. 9(b) [which is the same result as Fig. 2(a)].

APPENDIX B: FINITE-TIME LYAPUNOV EXPONENTS IN THE OPTOELECTRONIC FEEDBACK SYSTEM

To show the universality of our findings in the Mackey-Glass model, we used a different model, i.e., the optoelectronic time-delayed feedback system [4,11]

$$\frac{dx(t)}{dt} = -x(t) + \beta \sin^2[x(t-\tau) - \varphi], \quad (\text{B1})$$

where β is the feedback strength and φ is the feedback phase. The second term in this equation represents electronic delayed feedback and τ is the delay time. These parameters are fixed to $\beta = 20$ and $\varphi = \pi/4$ in our numerical simulations. The time t and the delay time τ are normalized with $\tau_0 = 2 \times 10^{-11}$.

Figure 10 show the standard deviation of the probability distribution of the finite-time Lyapunov exponents as a function of the delay time τ in the optoelectronic feedback system. The results show the power-law scaling and the scaling exponent $q = 0.50$ is obtained with τ^{-q} for $L = 1$ in Fig. 10. For other cases, we can observe the distortion of the power-law scaling at the region $L \approx \tau$, which can be also found in the Mackey-Glass model. The scaling exponents $q \approx 0.5$ are obtained for other regions except for $L \approx \tau$. These results show that the probability distribution of the finite-time Lyapunov exponents in the optoelectronic feedback system shows behavior similar to that in the Mackey-Glass model.

-
- [1] J. D. Farmer, *Physica D* **4**, 366 (1982).
[2] K. Pyragas, *Phys. Rev. E* **58**, 3067 (1998).
[3] M. C. Soriano, J. García-Ojalvo, C. R. Mirasso, and I. Fischer, *Rev. Mod. Phys.* **85**, 421 (2013).
[4] L. Larger and J. M. Dudley, *Nature (London)* **465**, 41 (2010).
[5] A. B. Cohen, B. Ravoori, T. E. Murphy, and R. Roy, *Phys. Rev. Lett.* **101**, 154102 (2008).
[6] A. Uchida, *Optical Communication with Chaotic Lasers, Applications of Nonlinear Dynamics and Synchronization* (Wiley-VCH, Weinheim, 2012).
[7] A. Uchida, K. Amano, M. Inoue, K. Hirano, S. Naito, H. Someya, I. Oowada, T. Kurashige, M. Shiki, S. Yoshimori, K. Yoshimura, and P. Davis, *Nat. Photon.* **2**, 728 (2008).
[8] L. Appeltant, M. C. Soriano, G. V. der Sande, J. Danckaert, S. Massar, J. Dambre, B. Schrauwen, C. R. Mirasso, and I. Fischer, *Nat. Commun.* **2**, 468 (2011).
[9] G. D. VanWiggeren and R. Roy, *Science* **279**, 1198 (1998).
[10] A. Argyris, D. Syvridis, L. Larger, V. Annovazzi-Lodi, P. Colet, I. Fischer, J. García-Ojalvo, C. R. Mirasso, L. Pesquera, and K. A. Shore, *Nature (London)* **438**, 343 (2005).
[11] R. Vicente, J. Dauden, P. Colet, and R. Toral, *IEEE J. Quantum Electron.* **41**, 541 (2005).
[12] K. Kanno and A. Uchida, *Phys. Rev. E* **86**, 066202 (2012).
[13] K. Kanno and A. Uchida, *Nonlinear Theory Appl. IEICE* **3**, 143 (2012).
[14] J. P. Eckmann and D. Ruelle, *Rev. Mod. Phys.* **57**, 617 (1985).
[15] H. F. von Bremen, F. E. Udawadia, and W. Proskurowski, *Physica D* **101**, 1 (1997).
[16] K. Geist, U. Parlitz, and W. Lauterborn, *Prog. Theor. Phys.* **83**, 875 (1990).
[17] S. Habib and R. D. Ryne, *Phys. Rev. Lett.* **74**, 70 (1995).
[18] G. Rangarajan, S. Habib, and R. D. Ryne, *Phys. Rev. Lett.* **80**, 3747 (1998).
[19] A. Wolf, J. B. Swift, H. L. Swinney, and J. A. Vastano, *Physica D* **16**, 285 (1985).
[20] P. Bryant, R. Brown, and H. D. I. Abarbanel, *Phys. Rev. Lett.* **65**, 1523 (1990).
[21] M. Sano and Y. Sawada, *Phys. Rev. Lett.* **55**, 1082 (1985).
[22] H. D. I. Abarbanel, R. Brown, and M. Kennel, *J. Nonlinear Sci.* **1**, 175 (1991).
[23] H. Abarbanel, R. Brown, and M. Kennel, *J. Nonlinear Sci.* **2**, 343 (1992).
[24] M. A. Sepúlveda, R. Badii, and E. Pollak, *Phys. Rev. Lett.* **63**, 1226 (1989).
[25] B. Eckhardt and D. Yao, *Physica D* **65**, 100 (1993).
[26] E. Aurell, G. Boffetta, A. Crisanti, G. Paladin, and A. Vulpiani, *Phys. Rev. Lett.* **77**, 1262 (1996).
[27] A. Prasad and R. Ramaswamy, *Phys. Rev. E* **60**, 2761 (1999).
[28] A. Prasad, V. Mehra, and R. Ramaswamy, *Phys. Rev. Lett.* **79**, 4127 (1997).
[29] A. Uchida, K. Yoshimura, P. Davis, S. Yoshimori, and R. Roy, *Phys. Rev. E* **78**, 036203 (2008).
[30] T. Mikami, K. Kanno, K. Aoyama, A. Uchida, T. Ikeguchi, T. Harayama, S. Sunada, K.-i. Arai, K. Yoshimura, and P. Davis, *Phys. Rev. E* **85**, 016211 (2012).
[31] F. T. Arecchi, G. Giacomelli, A. Lapucci, and R. Meucci, *Phys. Rev. A* **45**, R4225 (1992).
[32] G. Giacomelli, R. Meucci, A. Politi, and F. T. Arecchi, *Phys. Rev. Lett.* **73**, 1099 (1994).
[33] G. Giacomelli and A. Politi, *Phys. Rev. Lett.* **76**, 2686 (1996).
[34] M. C. Mackey and L. Glass, *Science* **197**, 287 (1977).